Production of Tb^{149} from Gold by 2.2-GeV Protons*

V. P. Crespo† and J. B. Cumming
Chemistry Department, Brookhaven National Laboratory, Upton, New York 11973

and

J. M. Alexander
Chemistry Department, State University of New York, Stony Brook, New York 11790
(Received 15 May 1970)

Angular distributions and differential range spectra at angles of 15, 60, 90, 120, and 165° to the beam direction have been measured for Tb^{149} recoiling from thin gold targets irradiated with 2.2-GeV protons. The observed mean velocities decrease monotonically from a value of 0.264 $(MeV/amu)^{1/2}$ at 15° to 0.149 $(MeV/amu)^{1/2}$ at 165°. The ratio of integrated intensity in the forward hemisphere to that backward is 3.10. The experimental results are consistent with the symmetry requirements of a two-step model for the reaction, provided that there is a positive correlation between $v_{\parallel}$, the forward component of velocity due to the first step, and V, the velocity due to the second step. However, there are substantial quantitative discrepancies between the experimental results and calculations based on the cascade-evaporation model which is commonly used to describe the two steps of a high-energy nuclear reaction. The calculations predict a value of $\langle v_{\parallel} \rangle$ twice as large as that observed and a much weaker correlation between V and $v_{\parallel}$. These effects are discussed in terms of possible contributions from heavy-fragment emission in both steps of the reaction. Systematics of the average energies of various recoil products suggest an empirical correlation that may be useful in distinguishing fission from "deep spallation."

I. INTRODUCTION

The production of Tb^{149} by high-energy proton irradiation of heavy-element targets has been the subject of a number of investigations.[1-5] The popularity of this nuclide is due to the ease with which it can be identified in the gross mixture of products. It has been noted[3] that Tb^{149} accounts for ≈99% of the total α activity observed in a gold foil several hours after the end of a high-energy proton irradiation. The high threshold (≈600 MeV) for the production of Tb^{149} from gold has led to the choice of this reaction as a monitor for high-energy proton beams.

In studies of high-energy nuclear reactions, Tb^{149} produced from Au^{197} is of interest as representative of a class of reactions which may be called "deep spallation," i.e., reactions leading to products far removed from the target nucleus which are not observed at bombarding energies below several hundred MeV. The excitation functions for such products rise rapidly in the energy region above 0.5 GeV in a manner similar to those of neutron-deficient fission products, e.g., I^{123} from uranium,[6,7] and of the so-called "fragmentation" products, e.g., Na^{24} from heavy-element targets.[8] Winsberg[2] has examined the recoil properties of Tb^{149} produced from Ta, Au, and Bi by protons of energies from 0.4 to 6 GeV. He used the thick-target–thick-catcher technique and also the thin-target–thin-catcher technique with 2π geometry. Winsberg concluded that the reaction mechanism, for a particular target, was essentially independent of energy and that the nucleons emitted to form Tb^{149} were, at least in part, bound in aggregates. The present investigation was undertaken to explore further the relationships among deep-spallation light-fragment production, and the low-momentum component of the spectrum of the neutron-deficient nuclide Ba^{131} produced from uranium by 2.2-GeV protons.[9] Rudstam and Sørenson[10] have proposed a spallation-like mechanism for the production of neutron-deficient iodine isotopes from uranium bombarded by 18-GeV protons. Alexander, Baltzinger, and Gazdik[6] have also suggested a connection between the neutron-deficient iodine isotopes and the light fragments.

In this paper are described measurements of range spectra at five angles and the angular distribution for Tb^{149} produced by the interaction of 2.2-GeV protons with gold. This work represents a continuation of studies[9,11-13] of momentum transfer to products from various reactions induced by high-energy protons. The experimental results are discussed in terms of the two-step vector representations developed by Sugarman and co-workers[14,15] and by Winsberg.[16] In this model the velocity $\vec{V}_L$ of a product in the laboratory system is described as the sum of the velocity $\vec{v}$ imparted to a nucleus by the first reaction step (prompt cascade) and $\vec{V}$, the velocity imparted by the second step (nuclear evaporation or fission). The angular distribution

of $\vec{V}$ is assumed to be symmetric about 90° to the beam direction in the moving system. It is not necessary to assume the validity of this two-step representation for the analysis of our results. However, it is convenient to initiate the analysis with such an assumption. The internal consistency of the observed angular distribution and velocity spectra provides a rather severe test of the two-step picture. Integral recoil experiments do not provide such tests, but they do yield various average quantities useful for testing reaction models.

II. EXPERIMENTAL PROCEDURES AND RESULTS

The procedures used in this experiment to measure range and angular distributions are similar to those described previously.[9] The main differences are due to the presence of recoils of rather short range and to the fact that chemical separation of terbium was not necessary prior to the assay of Tb^{149}. Targets used in this work were prepared by vacuum deposition of Au to a thickness of $\approx 8\ \mu g/cm^2$ onto ≈ 50-$\mu g/cm^2$ Formvar supporting foils. In some irradiations, ≈ 30-$\mu g/cm^2$ targets were used. The results showed no consistent pattern which could be ascribed to finite target thickness. Irradiations in the internal 2.2-GeV circulating proton beam of the Brookhaven Cosmotron were usually about 4 h in duration, and the integrated circulating beam was about 10^{14}–10^{15} protons. Multiple traversals of the target increased the effective beam intensity by a factor the order of 1000.[17]

The diameter of the catching foils was ≤ 3.8 cm, so that the entire sample could be placed into an α proportional flow counter. Because of the 4.1-h half-life, the rather low counting rates, and the number of samples, up to 10 counters were used. Their efficiencies were intercompared, and their daily performance was checked with thick uranium standards. Decay curves starting 1 h from the end of irradiation indicated that the dominant species in the samples was Tb^{149}. When counting was started earlier, a short-lived component, probably 18-min Dy^{151}, was also observed. We observed no source of Tb^{149} other than the gold target; hence, no blank corrections were necessary.

A. Angular Distribution and 2π Measurements

Catcher foils for the angular-distribution measurements were Al foils of thickness 1.7 or 1.2 mg/cm^2. Rectangular strips of this Al were laid on a cylindrical bed at a distance of 15 cm from the target. A Mylar mask, thicker than the range of the Tb^{149} recoils, covered the foil stack. Six apertures in the Mylar mask, each 3.8 cm in diameter, served to define areas of collection with ±7° resolution centered at angles of 15, 30, 45, 60, 75, and 90° to the beam direction. For the backward angles, the catcher assembly was rotated to collect at angles from 90 to 165°. After irradiation, the collecting areas were cut apart and the α activity from Tb^{149} was measured. As the catcher foils had appreciable thickness compared with the range of the α particles, the radiations were assayed separately from each side of each foil. Averaging the activity of the two sides serves to correct, to a very good approximation, for the variation of the penetration depth of the Tb^{149} recoils with angle. When the thicker foil was used, no Tb^{149} was detected in a layer of foil behind the first. With the 1.2-mg/cm^2 catchers, significant penetration of the first catcher occurred, and it was necessary to sum the activities of first and

TABLE I. Intensity per unit solid angle as a function of angle in the lab system for Tb^{149} recoils produced from gold by 2.2-GeV protons.

Angle (deg)	Ref. a	Ref. a	Ref. b	Ref. c	Ref. c	Weighted means
15	2.373	•••	2.308	•••	2.337	2.342
30	2.063	•••	2.147	•••	2.139	2.126
45	1.813	•••	1.839	•••	1.817	1.820
60	1.474	•••	1.470	•••	1.460	1.465
75	1.093	•••	1.071	•••	1.117	1.106
90	0.863	0.837	0.852	0.831	0.820	0.833
105	•••	0.592	•••	0.611	•••	0.607
120	•••	0.466	•••	0.454	•••	0.456
135	•••	0.370	•••	0.365	•••	0.365
150	•••	0.308	•••	0.310	•••	0.310
165	•••	0.274	•••	0.272	•••	0.272

[a] ≈ 8-μ/cm^2 target, ≈ 1.2-mg/cm^2 catchers.
[b] ≈ 8-μ/cm^2 target, ≈ 1.7-mg/cm^2 catchers.
[c] ≈ 30-μ/cm^2 target, ≈ 1.2-mg/cm^2 catchers.

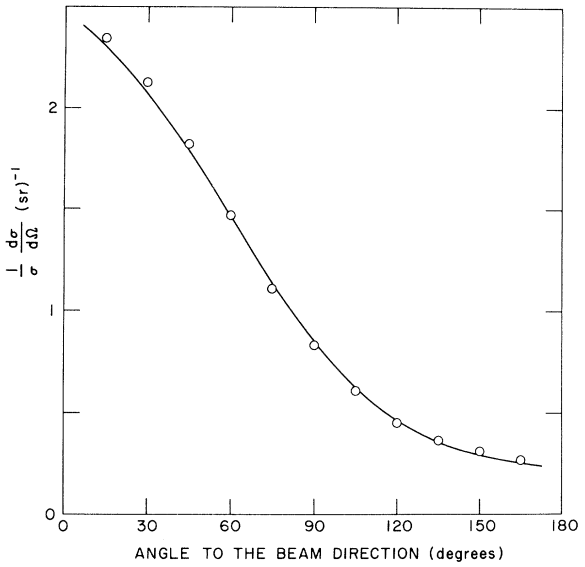

FIG. 1. Angular distribution in the lab system of Tb^{149} recoils from the irradiation of gold with 2.2-GeV protons. Points are from the experiment; the curve is calculated assuming a two-step mechanism for the reactions. (See text.)

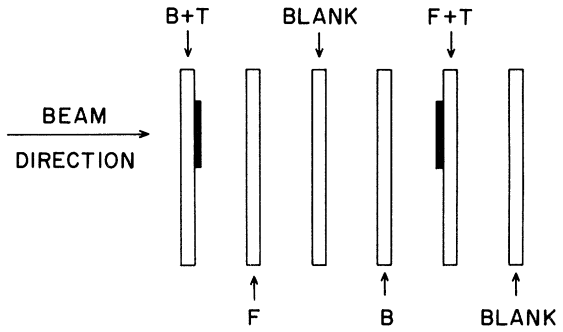

FIG. 2. Schematic diagram of the target and catcher arrangement for the 2π experiments. Targets are shown as solid areas, catchers are open. During irradiation the foils were in contact. The symbols F, B, and T denote the fraction of the Tb^{149} activity which is found in the forward and backward catcher or is retained in the target, respectively.

second catchers to obtain the total intensity at a particular angle.

Results of three experiments with the catchers oriented at forward angles and of two experiments at backward angles are presented in Table I. In reducing the observed counting data, it was assumed that each of the triplicate or duplicate experiments had arbitrary normalization factors. These factors were varied in an iterative procedure to minimize the weighted sum of squares of deviations from the weighted mean value at each angle. This led to weighted mean values of the recoil intensities at each angle in the forward hemisphere and also in the backward hemisphere. The forward distribution and backward distribution were joined at 90°. Over-all normalization of the results in Table I is such that integration over all space gives the value 4π. Based on agreement between triplicates or duplicates, the precision of the mean values of intensity per unit solid angle is ≈1%. There is no indication in Table I that the use of thicker targets resulted in a significant distortion of the angular distribution.

The angular distribution, plotted in Fig. 1, is strongly forward peaked. The intensity of recoils at 0° is approximately a factor of 10 higher than that at 180°. The ratio of the fraction of recoils found in the forward hemisphere, F, to the fraction found in the backward hemisphere, B, is 3.14 ± 0.05.

To check this value of F/B and to investigate retention of recoils by the targets, two experiments were performed with 1.7-mg/cm^2 Al catcher foils in a 2π geometry. As shown in Fig. 2, the assembly in the beam contained two independent target and catcher sets; hence, it was possible to evaluate F, B, and T, where T is the fraction of recoils retained in the target. Results listed in Table II indicate that T is quite low and that results from the angular distribution and 2π experiments are in good agreement. The quantity $F-B$ of Table II is approximately equal, in the two-step picture, to the quantity $\langle v_{\parallel}/V\rangle = \langle n_{\parallel}\rangle$ if $v_{\parallel} < V$ for all cases. The mean value of F/B from the angular distribution and 2π measurements is 3.10 ± 0.03.

TABLE II. Parameters obtained from the angular distribution and 2π measurements.

Source	Targets (μg/cm^2)	F	B	T	$(F-B)$
Angular distribution	8 and 30	0.759 ± 0.003	0.241 ± 0.003	...[a]	0.517 ± 0.006
2π (irradiation 1)	19	0.757 ± 0.004	0.243 ± 0.003	0.000 ± 0.006	0.515 ± 0.006
2π (irradiation 5)	8	0.745 ± 0.004	0.246 ± 0.004	0.009 ± 0.006	0.499 ± 0.006
Mean		0.755 ± 0.002	0.243 ± 0.002		0.510 ± 0.003

[a] T was assumed to be zero in the analysis of the angular distribution.

B. Velocity Spectra

Range distributions of the Tb^{149} recoils were measured at five angles to the beam direction in a series of 10 experiments. Eight of these experiments provided data at angles of 15, 90, and 165°; single experiments were performed at 60 and 120°. The thin catcher foils in these experiments were prepared from Formvar and were supported on aluminum rings. The recoil collection geometry was restricted by an aluminum baffle to a cone of half angle 6° centered on the desired angle. The thickness of each individual foil and its uniformity were measured with an α-particle thickness gauge.[18]

Experimental range-energy relationships are available[19-21] for Sm^{142}, Tb^{149}, and $Dy^{149,150,151}$ in aluminum. In order to relate the range data in Formvar to those in Al, we have performed single experiments at 15 and 90° with aluminum-leaf catcher foils. By comparing results of these measurements with those obtained with the Formvar catchers at the same angles we determined the stopping-power for Tb^{149} recoils of Formvar relative to that of aluminum. The range (in units of mg/cm^2) in aluminum, R_{Al}, is related to the range in Formvar, R_F, by the equation

$$\ln R_{Al} = 0.2642 + 1.096(\ln R_F) + 0.0257(\ln R_F)^2 \quad (1)$$

for values of R_F greater than 0.154 mg/cm^2. For smaller values of R_F we have used a constant ratio, $R_{Al}/R_F = 1.186$. The trend of relative stopping given by Eq. (1) is also observed in the energy-loss measurements of Moak and Brown[22] for iodine ions stopped in carbon and aluminum. Only slight changes would be made in the velocity spectra by use of a constant range ratio, $(R_{Al}/R_F) = 1.22$, and our conclusions would be unaffected. Use of aluminum catchers in all of our measurements would have given much poorer velocity resolution.

For the conversion of ranges in aluminum to velocities V_L or kinetic energies E we have used the relations:

$$\ln E = 2.460 + \ln R_{Al}, \quad (2)$$

when $R_{Al} \leq 0.279$ mg/cm^2, and

$$\ln E = 2.703 + 1.325 \ln R_{Al} + 0.105(\ln R_{Al})^2, \quad (3)$$

when $R_{Al} > 0.279$ mg/cm^2. These equations were obtained by least-squares fitting of experimental data from heavy-ion bombardments[19-21] and are estimated to be reliable to a few percent. For comparison, Winsberg[2] used the relation $\ln E = 2.511 + \ln R_{Al}$ in the analysis of his data.

Some of the results obtained from this series of range measurements are presented in Fig. 3 as velocity spectra; curves have been drawn to show the general trends. It may be seen that the spectra change smoothly with angle of observation. The low-velocity recoils [0.05 (MeV/amu)$^{1/2}$] are nearly isotropic in the lab system, while those of high velocity are strongly forward peaked.

We have attempted to fit the semilog plots of the velocity spectra with various polynomials by the least-squares method. The spectra can be fitted reasonably well by quartic equations. While there is no theoretical significance to be attached to the equations, they do permit a quantitative measurement of the scatter of the points about a smooth curve. Such analysis indicates that experiments 6, 19, and 20 are significantly poorer than the others. There were mechanical problems with targeting and foil counting in experiments 6 and 10. Misbehavior of some of the α counters was noted during experiments 19 and 20. We feel that these effects may make the spectra from those experiments somewhat ragged and that the mean velocities or energies should be given less weight in those cases.

Mean velocities and energies as determined in each of the experiments are listed in Table III along with average values where more than one determination was performed. From the agreement of the duplicate or triplicate measurements we conclude that the precision of a mean-velocity measurement having unit weight is 2.3%. For the energies, the precision is 3.7%. The dependence of average mean

TABLE III. Mean velocities and energies of Tb^{149} recoils from gold targets irradiated with 2.2-GeV protons, as determined from the range measurements.

Angle (deg)	Experiment	Mean velocity $\langle V_L \rangle$ (MeV/amu)$^{1/2}$	Mean energy $\langle T \rangle$ (MeV)
15	13	0.263	6.13
	16	0.264	6.19
	18	0.267 [a]	6.34
	⟨av⟩	0.264 ± 0.004	6.16 ± 0.16
60	19	0.234 [b]	5.00 [b]
90	6	0.202 [b]	3.87 [b]
	9	0.214 [a]	4.20 [a]
	10	0.215 [b]	4.27 [b]
	17	0.218	4.38
	⟨av⟩	0.213 ± 0.004	4.22 ± 0.11
120	20	0.184 [b]	3.23 [b]
165	12	0.144	2.08
	14	0.152	2.28
	15	0.151	2.20
	⟨av⟩	0.149 ± 0.002	2.20 ± 0.05

[a] These values, obtained with aluminum catchers, were not included in calculating the averages, because they were used to fix range-energy parameters.

[b] In calculating the averages, these values were given weight $\frac{1}{2}$. These experiments suffered from certain difficulties mentioned in the text.

velocity and average mean kinetic energy on angle of observation is shown in Fig. 4. Error flags in this figure reflect the precision only. Accuracy of the average values depends largely on the range-energy data used in obtaining Eqs. (2) and (3). We believe that reasonably conservative estimates of the accuracies of the average velocities and energies are 2.5 and 5%, respectively. The sigmoid-shaped curves in Fig. 4 were calculated by the fitting procedure which will be described below.

III. ANALYSIS OF RESULTS

There are two general approaches to the analysis and discussion of kinetic data such as we have presented above. The first method starts with the assumption of only the general features of a two-step model for the reaction and then searches for a set of velocity parameters, i.e., spectra of $\vec{V}$ and $\vec{v}$ as well as correlations between $\vec{V}$ and $\vec{v}$, which can reproduce the experimental data. Failure to find such a set is taken as indicating a breakdown of the two-step model. However, if a satisfactory fit is achieved, the significance of the derived parameter set is investigated by comparison with calculations using specific models for the two steps which together describe the over-all reaction. The second method is to calculate, from a completely detailed reaction model, a set of predictions for measurable velocity and angular distributions. Such predictions can then be compared directly with the experimental data. These two approaches are not mutually exclusive in any sense and both should be employed in order to interpret the measurements.

There is some advantage to the first method insofar as the validity of the two-step model can be tested and some general features of the reaction can be deduced without initially depending on the detailed calculations for each step. We start our analysis along this path by assuming that a two-step model is appropriate. That is, we assume that each velocity in the lab, $\vec{V}_L$, can be resolved into two components, $\vec{v}$ imparted by the fast intranuclear cascade step and $\vec{V}$ imparted by the slower evaporation or fission step. The velocity vector $\vec{v}$, cylindrically symmetric about the beam direction, may be resolved into components $v_\parallel$ and $v_\perp$, parallel and perpendicular to that axis. The angular distribution of the velocity $\vec{V}$ must have reflection symmetry about a plane normal to $\vec{v}$. Since $\vec{v}$ is cylindrically symmetric about the beam, this means that the angular distribution of all $\vec{V}$ vectors must also be symmetric about a plane normal to the beam axis. A convenient form in cases where the anisotropy (as measured by the value of b/a) is small is given by,

$$W(\theta) = (a + b\cos^2\theta)/(a + \tfrac{1}{3}b), \tag{4}$$

where θ denotes the angle between $\vec{V}$ and the beam.

With only these symmetry assumptions one can show that

$$\langle v_\parallel \rangle = \langle\langle V_L \cos\theta_L \rangle\rangle \tag{5}$$

and

$$\langle v^2 + V^2 \rangle = \langle\langle V_L{}^2 \rangle\rangle \ . \tag{6}$$

With the further restriction $b/a = 0$, it follows that

$$\langle v_\perp{}^2 + \tfrac{2}{3}V^2 \rangle = \langle\langle (V_L \sin\theta_L)^2 \rangle\rangle \tag{7}$$

and

$$\langle v_\parallel{}^2 + \tfrac{1}{3}V^2 \rangle = \langle\langle (V_L \cos\theta_L)^2 \rangle\rangle \ , \tag{8}$$

where V_L is the magnitude of the laboratory velocity observed at angle θ_L to the beam. Similarly, V is the magnitude of the vector $\vec{V}$ in the frame of reference moving at velocity $\vec{v}$. The double average symbols indicate averaging over both θ_L and V_L. Equations (7) and (8) are not greatly in error[23] for small nonzero b/a values. The average quantities defined by Eqs. (5) to (8) have been obtained from the measurements and are given in Table IV. They can, of course, be directly compared with model results, or they can serve as bench marks for more elaborate calculations. We will use them in both ways.

It is clear from Fig. 3 that the lab velocity distributions are very broad for this reaction. In fact, this great breadth is the general characteristic of "deep spallation" reactions which makes them difficult to study and difficult to analyze. One must expect that the distributions of v and V will also be very broad and therefore many of the simplifying approximations may not be valid.[24] This situation has led us to employ an "inverse calculation" based on assumed distributions of $\vec{v}$, V, and $W(\theta)$ which generates distributions of $\vec{V}_L$. These distributions were then compared with the experimental data, new distributions were assumed, and new comparisons made. This iterative method of fitting the data is straightforward for narrow velocity distributions as has been previously described.[9] However, for

TABLE IV. Values for means of various two-step model parameters obtained from data of the present experiment.

Quantity	Value
$\langle v_\parallel \rangle$	(0.0923 ± 0.0037) $(\mathrm{MeV/amu})^{1/2}$
$\langle v_\perp{}^2 + \frac{2}{3}V^2 \rangle$	(0.0377 ± 0.0014) MeV/amu
$\langle v_\parallel{}^2 + \frac{1}{3}V^2 \rangle$	(0.0269 ± 0.0009) [a] MeV/amu
$\langle v^2 + V^2 \rangle$	(0.0646 ± 0.0023) [a] MeV/amu
$\langle v_\parallel / V \rangle$	(0.510 ± 0.003) [a,b]

[a] b/a assumed to be zero.

[b] All values of $v_\parallel/V$ assumed to be ≤ 1.

broad distributions the variety of assumptions which must be tried tends to obscure the results behind questions of uniqueness and accuracy. These questions are important, to be sure, but are better discussed after the calculated distributions are fitted to the data and the assumed distributions of $\vec{V}$ and $\vec{v}$ are before us.

We proceed to describe a search for one set of values of $\vec{v}$, V, and $W(\theta)$ which is consistent with our data. Then we will indicate the nature of other possible sets, and we will discuss the results as they relate to the nucleonic cascade and to the evaporation models. We assume initially that there is a unique relationship between $v_{\parallel}$ and V, that $v_{\perp}$ is zero, and that $\vec{V}$ is isotropic with a distribution essentially the same as that observed at $\theta_L = 90°$. The distributions were adjusted to be consistent with average quantities $\langle v_{\parallel} \rangle$ and $\langle V^2 + v^2 \rangle$ from Table IV. The relationship between $v_{\parallel}$ and V was taken as

$$\frac{v_{\parallel} - \langle v_{\parallel} \rangle}{\langle v_{\parallel} \rangle} = n \frac{V - \langle V \rangle}{\langle V \rangle} \quad . \tag{9}$$

Velocity distributions in the laboratory were then generated by a Monte Carlo method, generally using 50 000 vector additions per calculation. The first comparison of calculation with experiment was rather poor, so a series of distributions of V were tried. Using the "best" of the V distributions, various nonzero values of $v_{\perp}$ (of the form $v_{\perp} = \alpha v_{\parallel}$) were then tried. Using the "best" V distribution and "best" $v_{\perp}$ values, the best value of n [from Eq. (9)] was the searched for. At this stage of the trial and error fitting, calculation was rather close to experiment but not within experimental uncertainties. A slightly modified spectrum of V was then chosen, and the other parameters were searched again. The two most sensitive features are the shape of the distribution of V (particularly the low-velocity region) and its correlation with $v_{\parallel}$ through the parameter n.

In Fig. 5 we show the dependence of the mean velocities at five lab angles and the F/B ratio on the quantity n in Eq. (9). The other parameters were held fixed as follows: spectrum of V as shown in Fig. 8 (to be discussed later) with $\langle V \rangle = 0.209$ (MeV/amu)$^{1/2}$; $\langle v_{\parallel} \rangle = 0.0943$ (MeV/amu)$^{1/2}$; $v_{\perp} = 0.6 v_{\parallel}$; $b/a = 0$. We see from Fig. 5 that it is possible with $n = 0.44$ to account for the mean velocities and the F/B ratio. More detailed comparisons of the velocity and angular distributions are shown in Figs. 1, 4, and 6. For these comparisons, 10^6 vector ad-

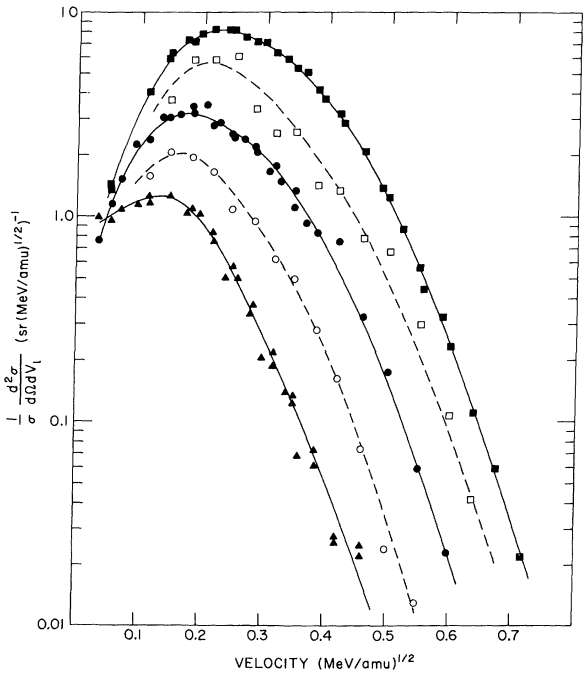

FIG. 3. Velocity spectra of Tb^{149} recoils from gold irradiated by 2.2-GeV protons. Small corrections for the experimental resolution have been applied. The curves are drawn free hand to indicate the general trends of the spectra. Angles of observation starting from the topmost curve and proceeding downward were 15, 60, 90, 120, and 165°. Normalization is such that integration of a given curve over velocity will give the intensity observed in the angular distribution.

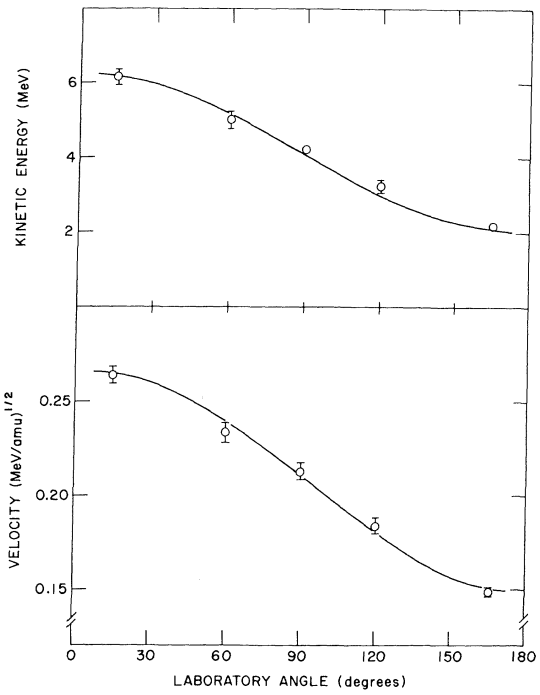

FIG. 4. Dependence of mean velocity and mean kinetic energy of Tb^{149} recoils on the angle of observation. The curves were calculated assuming a two-step model as described in the text.

ditions were performed with the final parameter set. The angular distribution is fitted quite well, and the general trends of the calculated velocity distributions are reproduced.

A question can be raised concerning the uniqueness of the spectra of $\vec{v}$ and $\vec{V}$ obtained by the above fitting procedure, in particular, about the identification of them with the first and second steps of the reaction, respectively. The significance of the terms in the vector equation, $\vec{V}_L = \vec{v} + \vec{V}$ must be given special consideration when applied to most recoil experiments, as the data obtained in such experiments cannot be analyzed on an event by event basis. Rather, the observed data, representing an average over all allowed combinations of v and V, are resolved into two components, one generally forward directed representing the average motion of the system after the first step, and a second component which is symmetric about 90° in this moving system. This symmetric component will certainly include a contribution from what can be considered the "isotropic" part of the first step.

We can, in principle, think of an observed velocity vector $\vec{V}_L$ as being resolvable into three components,

$$\vec{V}_L = \langle \vec{v} \rangle + \Delta\vec{v} + \vec{V} , \tag{10}$$

where the term $\langle \vec{v} \rangle$ describes the mean motion of those cascade nuclei which are progenitors of the observed product. Its components are $\langle v_{\parallel} \rangle$ and $\langle v_{\perp} \rangle$. The second term $\Delta\vec{v}$ takes into account deviation from the mean in each individual cascade event. Monte Carlo calculations[25] lead us to expect comparable magnitudes for $\langle \vec{v} \rangle$ and $\Delta\vec{v}$. The third term in Eq. (10), $\vec{V}$, is the true contribution from the second step of the reaction. As the symmetry properties of $\Delta\vec{v}$ are very similar to those of $\vec{V}$, they cannot be resolved in most recoil experiments, and what is obtained is an effective value which includes both terms. We can think of three general situations when discussing Eq. (10). In fission, the vector $\vec{V}$ normally dominates the other terms, and any error due to $\Delta\vec{v}$ will be small. At the other extreme, in some reactions [e.g., a $(p,p\pi^+)$ reaction[26] or possibly the production of Na^{24} from bismuth[12]] there may be no $\vec{V}$ or only a small contribution from it. In this case, although it might be formally

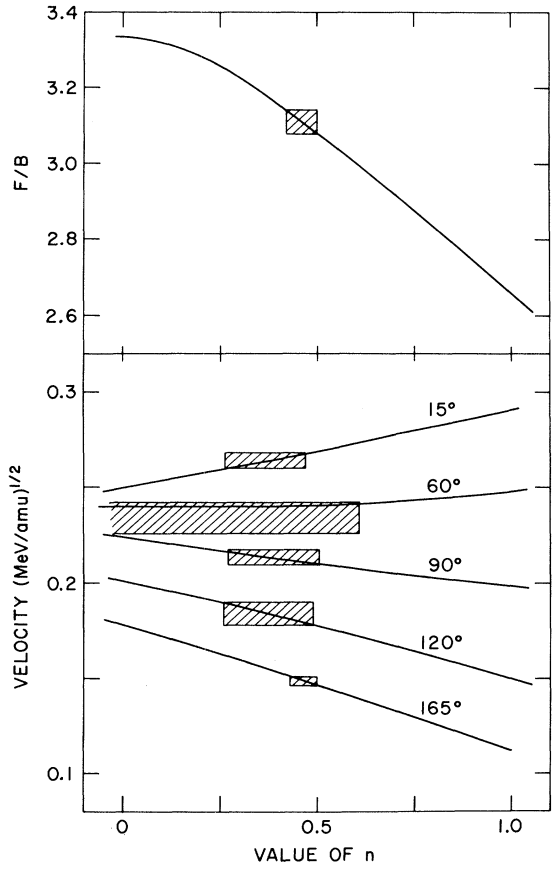

FIG. 5. Dependence of calculated mean velocities and the F/B ratio for Tb^{149} on the value of n in the assumed correlation function, $(v_{\parallel} - \langle v_{\parallel} \rangle)/\langle v_{\parallel} \rangle = n(V - \langle V \rangle)/\langle V \rangle$. The shaded boxes denote regions consistent with the experimental values.

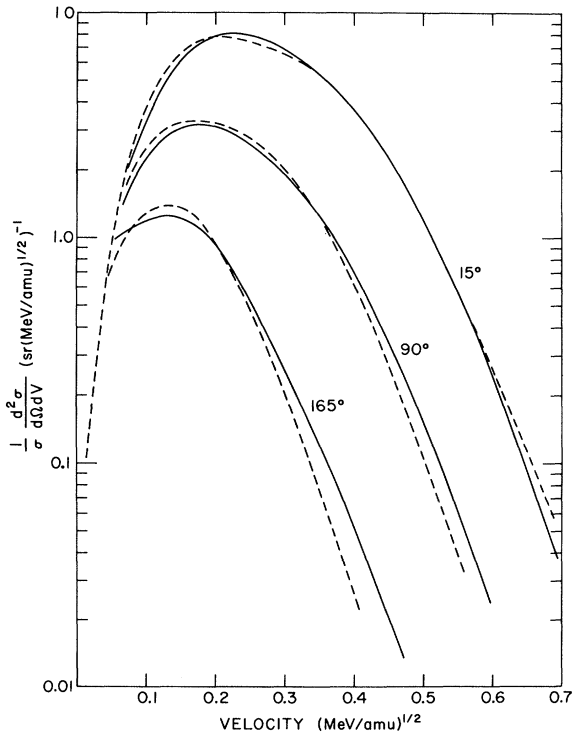

FIG. 6. Comparison of experimental (solid curves) with calculated velocity spectra of Tb^{149} produced from gold by 2.2-GeV protons. The calculated (dashed) curves were obtained using the two-step model described in the text.

possible to analyze an experiment in terms of two steps, this would not be significant, as the product momentum is determined primarily by the cascade. The third situation which probably includes "deep spallation" is intermediate between these extremes with comparable contributions from the three terms. In this case, a contribution from the cascade momenta to the spectrum deduced for V is expected.

What then have we achieved through our fitting procedure? First we have shown that there is no obvious discrepancy with a two-step model, in contrast to the case of Na^{24} produced from Bi^{209} [12] Secondly, we have obtained values of certain average quantities and certain limits on the sorts of spectra of v and V which can reproduce the experiments.

IV. DISCUSSION

A. Production of Tb^{149}

As described in the preceding section, the observed velocity spectra and angular distribution of Tb^{149} recoils can be fitted by a calculation assuming a two-step mechanism [a fast step followed by a slow step with the relationship between steps expressed in Eq. (9)]; hence, there is no direct evidence for contributions from a one-step fast mechanism. Within the framework of this two-step model, further insight into the parameters for Tb^{149} production is provided by comparison of the measured quantities with those of currently available calculations for the assumed two steps of the reaction.

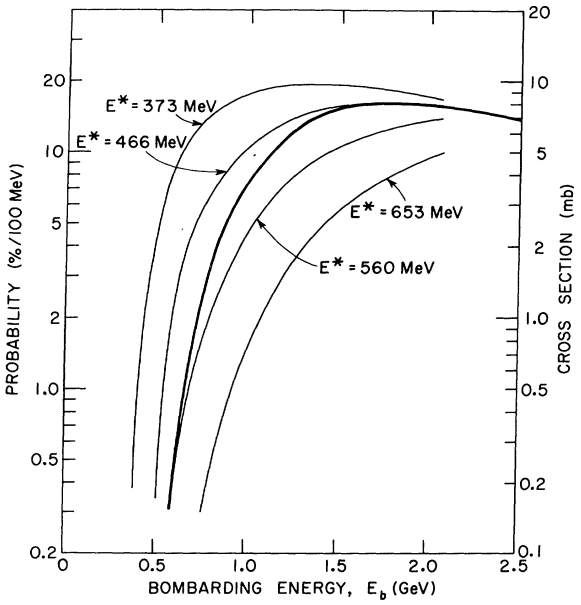

FIG. 7. The excitation function for Tb^{149} production from gold (Refs. 4 and 30) compared with the probability for depositing various excitation energies E^* in the prompt intranuclear cascade. The spectra of E^* values were obtained from Monte Carlo calculations (Ref. 25).

The primary information from this experiment on the first step of the reaction is contained in the value given in Table IV for $\langle v_{\parallel} \rangle$, the forward component of velocity of those post-intranuclear-cascade nuclei which ultimately deexcite to the observed product. Estimates of $\langle v_{\parallel}^2 \rangle$ and $\langle v_{\perp}^2 \rangle$ may also be obtained from the data in Table IV if a value for $\langle V^2 \rangle$ can be found in some other way. In addition, the observation that the fitting procedure, as described in Sec. III above, was not significantly improved by including an anisotropic distribution for $\vec{V}$, i.e., nonzero values for b/a in Eq. (4), indicates that there is no strongly preferred orientation of angular momentum vectors in the post-cascade nuclei, or that the second deexcitation step is insensitive to such orientation if produced. Isotropic distributions of $\vec{V}$ have also been reported[9] for Ba^{131} and Pd^{103} formed in the fission of U by 2.2-GeV protons. Values of $\langle v_{\parallel} \rangle$ for these reactions are comparable with the value for Tb^{149} production from gold. At a bombarding energy of 2.2 GeV, we conclude that no preferred angular momentum orientation is produced by those intranuclear cascades which, on the average, transfer about 20% of the incident proton's momentum to the struck nucleus.

The significance of the value of $\langle v_{\parallel} \rangle$ obtained in the present experiment is best discussed in terms of the mean excitation energy $\langle E^* \rangle$ of those post-cascade nuclei which will ultimately deexcite to form Tb^{149}. As has been noted by Porile,[27] the Monte Carlo calculations[25] of intranuclear cascades show a correlation between E^* and the mean value of $v_{\parallel}$ at a particular value of E^*. This correlation appears remarkably insensitive to target, bombarding energy, or nuclear model used in the calculation.[28] From the data of Metropolis *et al.*[25] for 1.84-GeV protons incident on Bi and U, we find this correlation can be expressed as

$$\langle v_{\parallel} \rangle / v_{CN} = 0.732 E^* / E_{CN}. \tag{11}$$

Here v_{CN} and E_{CN} are the velocity and excitation energy, respectively, which would have resulted if the incident particle had amalgamated with the target nucleus. There is no significant difference between the proportionality factors for the Bi and the U data considered separately, nor is there a significant nonzero intercept in the correlation line. Using this relation we find $\langle E^* \rangle$ for Tb^{149} production from gold by 2.2-GeV protons to be 300 MeV. Winsberg's[2] results from 0.7 to 6.2 GeV give an $\langle E^* \rangle = 243$ MeV, with no significant dependence on the energy of the bombarding particle. Little if any energy is available for kinetic energy of the

evaporated particles, as the binding energy necessary to remove 48 separate nucleons from Au^{197} to form Tb^{149} is 335 MeV. This has been interpreted by Winsberg[2] as indicating that the emission of some larger fragments must play a role in Tb^{149} production.

Porile and Sugarman[29] have described a different method for estimating $\langle E^* \rangle$, which is based on an analysis of the excitation function for a particular product in terms of the deposition energy spectra obtained from Monte Carlo calculations. We have obtained spectra of excitation energies of the post-cascade nuclei for bombarding energies from 0.4 to 2.0 GeV by interpolation and small extrapolations from the results of Metropolis *et al.*[25] for 0.46-, 0.93-, and 1.83-GeV protons incident on Bi^{209}. The dependence of probability of several selected E^* values on bombarding energy is shown by the light lines in Fig. 7. (These are based on E^* bins of 93-MeV width centered at the indicated energies.) The experimental excitation function[30] for Tb^{149} production is shown by the heavy line in Fig. 7. The Porile-Sugarman procedure[29] is equivalent to representing this excitation function as a linear combination of the E^* excitation functions in which the coefficients representing the contribution of the various E^* values to Tb^{149} production are independent of energy. We have not been able to find such an energy independent combination which can account both for the rapid rise of the Tb^{149} cross section as the proton energy is increased from 0.6 to 1 GeV and for the peak in the experimental excitation function at ≈1.8 GeV. However, considering possible errors in the assumptions of this method of analysis or from the Monte Carlo calculations, it seems reasonable to say the shape of the observed excitation function suggests that the mean value of E^* for Tb^{149} production from gold is about 500 MeV. It is clear that a value as low as the 300 MeV deduced from the observed forward momentum transfer is incompatible with the shape of the excitation function.

It might be argued that this discrepancy could be due to the fact that Tb^{149} is produced by reactions which are in some way atypical and that any analysis based on Monte Carlo calculations for "average" products is invalid. However, the 7.4-mb cross section for Tb^{149} production from gold at 2.2 GeV does not appear unusually low for a typical spallation product. Furthermore, a discrepancy of the same type has been noted in a recent study[31] of the fission of uranium by 2.9-GeV protons in which semiconductor detectors were used to detect fission fragments in coincidence. From the angular correlation of the fragments (which is related to $\langle v_{\parallel} \rangle$), a value of $\langle E^* \rangle$ was deduced which was lower than that estimated from the mean mass of the fragments. The discrepancy between $\langle E^* \rangle$ values from recoil studies and those from excitation-function measurements also manifests itself in the strange proton energy dependence of $\langle E^* \rangle$ values for neutron-deficient Pd isotopes formed from uranium. The recent results of Panontin and Porile[32] show an apparent decrease of $\langle E^* \rangle$ as the proton energy is increased from 450 MeV to 12 GeV. These discrepancies can be accounted for if the older Monte Carlo calculation[25] at GeV energies (or the method used to derive a $\langle v_{\parallel} \rangle$-$E^*$ relationship from its output) generally overestimates the value of $\langle v_{\parallel} \rangle$ associated with a particular value of E^*. Resolution of this question must await extension of the more detailed recent Monte Carlo calculations[28] into the GeV region. At this time it would appear to be extremely unwise to draw any strong conclusions which depend on E^* values deduced from $\langle v_{\parallel} \rangle$ measurements at GeV energies.

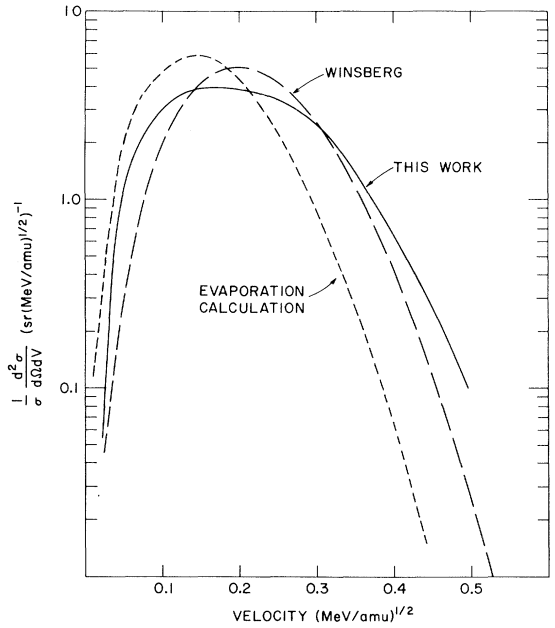

FIG. 8. Comparison of spectra of V. The solid curve is that used in the present work to fit the experimental data on Tb^{149} production from gold. The long-dashed curve is that used by Winsberg, Ref. 2. The short-dashed curve is that predicted by an evaporation calculation (see text and Ref. 33).

We now turn to the consideration of nuclear evaporation after the prompt cascade is assumed to be complete. The spectrum of V (obtained by the fitting procedure described above) is shown as the solid line in Fig. 8. The long-dashed line in this figure is the spectrum deduced by Winsberg[2] from his 2π range measurements. Even though the shapes are rather different, the mean values of V differ by only 3%. To obtain spectra for compari-

son, Re^{186} was selected as a representative post-cascade nucleus and 1000 evaporation cascades were calculated by a Monte Carlo procedure starting from this nucleus at each of three excitation energies, 400, 500, and 600 MeV. These calculations were kindly performed by Porile using programs developed by him and described elsewhere.[33] The calculations included the emission of the usual light particles up to He^4 and simulated heavier-fragment emission by inclusion of Li^7 with an enhanced statistical weight. As expected, the length of the evaporation cascades was observed to increase with increasing excitation energy, the mean cascade length corresponding to an average expenditure of ≈15 MeV for each nucleon lost. Some results of these calculations are listed in Table V. Evaporation cascades leading to mass 149 are seen to be rare events for $E^* = 400$ MeV. It can be concluded that mass 149 would be the most probable product (the residue of ≈13% of the cascades) at an excitation energy of about 550 MeV, in agreement with the conclusion drawn from our analysis of the experimental excitation function.

Calculated mean recoil velocities $\langle V \rangle$ and mean kinetic energies $\langle T \rangle$, as shown in Table V, are substantially lower than the values deduced by our fitting procedure. The apparent decrease of the calculated values as the excitation energy increases is not statistically significant. In general, for a given excitation energy, the calculated recoil velocity increased with increasing length of the evaporation cascade. However, rather to our surprise, if the cascade length is fixed by selecting a particular mass product, the recoil velocity is essentially independent of excitation energy. We can infer that the model predicts that increased excitation energy leads in part to breaking up nucleon aggregates, rather than solely to increased kinetic energy of the emitted particles.

The spectrum of recoil velocities calculated for products having masses 148, 149, and 150 is shown as the short-dashed line in Fig. 8. Results for all three excitation energies have been combined to improve statistical accuracy. The calculated curve significantly underestimates the number of high-velocity recoils when compared either with the spectrum deduced by Winsberg[2] or that from the present work. We conclude that the evaporation model including emission of particles up to Li^7 cannot account for the spectrum of V deduced by the fitting procedure if the calculation is performed for *stationary starting nuclei.*

Initially we had explored the rather attractive idea that the missing high velocities were evidence for the emission of particles even heavier than Li^7 in some of the events. The observed spectra[12] and mean momenta[34] of Na^{24} emitted during high-energy nuclear reactions with heavy-element targets would just supply such recoil kicks to Tb^{149}. However, we must recall that the fitting procedure we have used tends to yield an effective spectrum of V [a combination of $\Delta\vec{v} + \vec{V}$ in Eq. (10)], which may contain contributions from the prompt-cascade step, whereas the calculated spectrum does not. Can the difference between fitted and calculated V spectra be due to very broad distributions of $v_\parallel$ and $v_\perp$?

To pursue this further, we will follow what we have called previously the second method of analysis, a complete calculation which adds the evaporation calculation to a detailed calculation of momentum transfer by the prompt cascade. We start from the output of the Monte Carlo calculations of Metropolis *et al.*[25] for 1.84-GeV protons incident on Bi and U. (Our conclusions are not changed by considering either element separately.) Following the procedure outlined by Porile,[27] the momentum of the product of each cascade was calculated using momentum conservation and the energies and directions of each particle emitted in the cascade. Because the Monte Carlo output did not preserve the sign of one of the direction cosines of the emitted particles in a direction perpendicular to the beam, a random choice of this sign was made. As has been noted,[33] this overestimates (on the average) the component of recoil momentum in that direction. For those cascades which ultimately give

TABLE V. Summary of evaporation calculations on Re^{186} and comparison with values deduced from experiments.

E^* (MeV)	Fraction of events giving mass 149	Most probable product mass (amu)	$\langle V \rangle$ (Ref. a) $(\text{MeV/amu})^{1/2}$	$\langle T \rangle$ (Ref. a) (MeV)
400	0.003	≈159	0.171	2.52
500	0.074	≈153	0.161	2.27
600	0.105	≈146	0.157	2.16
This experiment [b]		•••	0.209	3.88
Winsberg [c]	•••	•••	0.215	3.90

[a] Averages for products of masses 148, 149, and 150 to give improved statistical accuracy.
[b] Values based on the fitting procedure described in the text.
[c] See Ref. 2.

mass 149, this mean momentum was 48% larger than the mean in the other perpendicular direction. We have multiplied all calculated momenta in the ambiguous direction by 0.677 to make the means equal. The over-all effect is to reduce the value of $\langle v_\perp \rangle$ by 20% compared with the uncorrected value.

The mass A and nuclear charge Z of each cascade product were appropriately shifted to correspond to production from a gold target. Each component of recoil velocity was multiplied by the factor 239/198 for uranium or 210/198 for bismuth targets, as the $v_\parallel/v_{CN}$ versus E^*/E_{CN} relationship is observed to be independent of target mass. This set of cascade nuclei were then used as starting points for an evaporation calculation in the following manner. A most probable mass loss by evaporation was calculated for each cascade product by dividing its excitation energy by 15 MeV/amu, the factor obtained from the calculations on Re^{186}. Since the most probable mass loss did not in general lead to a final product at mass 149, it was necessary to know the probabilities of various fluctuations about the most probable. These were also obtained from the Re^{186} calculations. With this procedure we were able to select from 1281 inelastic events, 440 of which could give significant yields at mass 149, and to assign to each of these events a probability which varied from 1 per 1000 to 132 per 1000 that it would deexcite to mass 149.

Some properties of this set of cascade nuclei which play a role in mass-149 production are shown in Fig. 9. The probability that intermediate nuclei of various masses yield mass 149 is shown in the lower part of this figure. The progenitors of mass 149 form a nearly Gaussian distribution about the most probable mass, 187.4. (We note our choice of Re^{186} was not too bad.) The total probability for forming mass 149 is ≈1.9% of the inelastic cross section,[35] or ≈31 mb. This is about a factor of 2 higher than predicted by the empirical yield systematics developed by Rudstam[36] and Schwarz and Oeschger.[37] In either case, the observed Tb^{149} cross section[30] at 1.84 GeV, 7.7 mb, is a significant fraction of the total mass-149 yield.

The mean excitation energies (weighted by the probability of mass-149 formation) are also shown in Fig. 9. Values of E^* increase from less than 500 MeV for the cascade nuclei nearest to mass 149 to over 600 MeV for those furthest removed. It is interesting to note that this trend is just the reverse of that observed if no selection as to final product is imposed. In that case, the longer prompt cascades lead to higher excitation energies. The over-all mean value of E^* for mass-149 production is 572 MeV, in reasonable agreement with that from the shape of the excitation function.

Weighted mean values of the parallel and perpendicular velocity components of the cascade nuclei are given in Fig. 9. The values of $\langle v_\parallel \rangle$ are seen to vary with mass of the intermediate nucleus in a manner parallel to that of $\langle E^* \rangle$. The perpendicular component $\langle v_\perp \rangle$ shows a slight trend in the reverse direction. The ratio of $\langle v_\perp \rangle$ to $\langle v_\parallel \rangle$ averaged over all events leading to mass 149 is 0.57, quite close to the value 0.6 used in our fitting procedure. However, the over-all average value of $\langle v_\parallel \rangle$ is 0.184, twice the value derived from our experimental data. This is, of course, just another reflection of the discrepancy in $\langle E^* \rangle$ values obtained from the experimental $\langle v_\parallel \rangle$ and the excitation-function shape.

To complete the calculation and obtain predicted velocity distributions in the lab system, we must add the second step of the reaction. To the vector

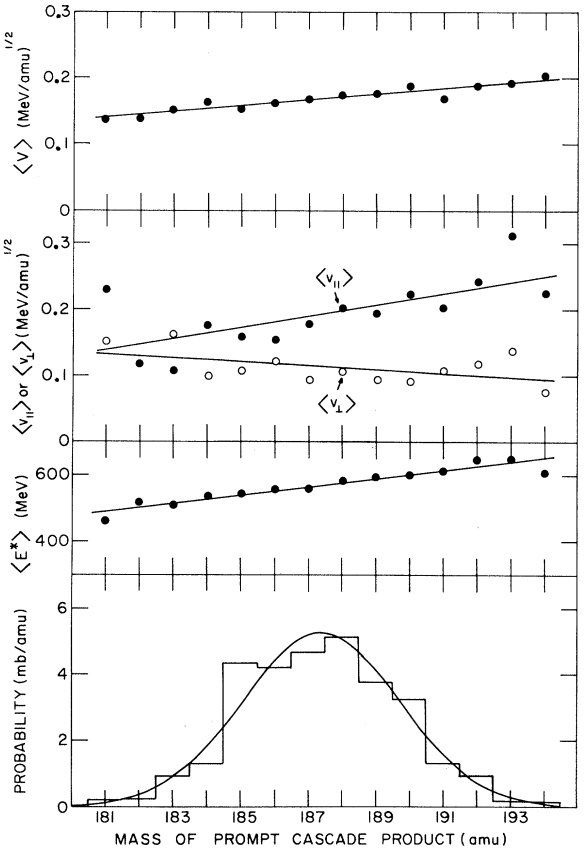

FIG. 9. Calculated results for the formation of mass-149 nuclei from gold irradiated by 1.84-GeV protons. From bottom to top are shown: the distribution in mass of the cascade nuclei which are progenitors of mass-149 nuclei, the average excitation ($\langle E^* \rangle$) of each of these, the mean forward ($\langle v_\parallel \rangle$) and perpendicular ($\langle v_\perp \rangle$) velocity components of these nuclei, and the mean velocity ($\langle V \rangle$) imparted to the final product by particle evaporation from the intermediate nucleus.

$\vec{v}$ of each of the selected cascades we have added a vector $\vec{V}$ for the evaporation step, the orientation of $\vec{V}$ being taken as isotropic. For each prompt cascade, the number of such vector additions was proportional to the probability that the particular cascade event was a progenitor of mass 149. (The actual number varied from 1 to 132.) In obtaining values for V we made use of the fact that the evaporation calculations on Re^{186} showed the spectrum of V for a given evaporation-cascade length ΔA, was virtually independent of E^*. Values of V were then selected so their frequency was proportional to the probability of their occurrence in the spectrum calculated for the ΔA value equal to the mass of the cascade nucleus minus 149. The entire set (23 796) of such calculations gives predictions for the angular distribution, velocity spectra, and the various mean values which may be compared with the experimental quantities. While this is not strictly speaking a complete calculation (we have taken a considerable shortcut in treating the evaporation step), we expect its output should be indistinguishable from a detailed calculation if the same evaporation model were used.

The experimental value of F/B and mean velocities at our five angles of observation are compared with those calculated in Table VI. Entries in the column headed Calc-1 are from the calculation just described. It predicts a value of F/B three times that observed, a direct consequence of the large value of $\langle v_{\parallel} \rangle$ from the prompt cascades. The calculation predicts that the cascade step will be the dominant factor in Tb^{149} production as the calculated value of $\langle v_{\parallel}/V \rangle$ is 1.39. This manifests itself in the very poor agreement (except at 90°) of the calculated and observed mean velocities. It is extremely unlikely we can reconcile these discrepancies by any small changes in either the prompt cascade or evaporation calculations. The main difficulty appears to be that the calculation of Metropolis *et al.*[25] at 1.84 GeV drastically overestimates forward momentum transfer.

TABLE VI. Comparison of some calculated recoil properties with those experimentally measured for Tb^{149} produced by the irradiation of gold with 2.2-GeV protons.

	Exp.	Calc-1 (Ref. a)	Calc-2 (Ref. a)
F/B	3.10 ±0.03	9.67	3.74
$\langle V_{15°} \rangle$	0.264±0.004	0.321	0.235
$\langle V_{60°} \rangle$	0.234	0.259	0.234
$\langle V_{90°} \rangle$	0.213±0.004	0.218	0.216
$\langle V_{120°} \rangle$	0.184	0.192	0.185
$\langle V_{165°} \rangle$	0.149±0.002	0.177	0.148

[a]The nature of these calculations is described in the text.

It may be of interest to see what other discrepancies remain when the major difference is removed by repeating the calculation with values of $v_{\parallel}$ reduced by a factor of 2 to force agreement between experimental and calculated values of $\langle v_{\parallel} \rangle$. Results from this revised calculation are given in the column of Table VI headed Calc-2. As could be anticipated, F/B has dropped and now is only 20% greater than the experimental value. The calculated mean velocities at angles from 60 to 165° reproduce the experimental values surprisingly well. Even the calculated standard deviation of the 90° spectrum, 0.089 $(\text{MeV/amu})^{1/2}$, is not very different from the observed value 0.106 $(\text{MeV/amu})^{1/2}$. Apparently a substantial part of the discrepancy between calculated and fitted spectra seen in Fig. 8 can be due to the inclusion of contributions from the first step of the reaction to the fitted spectrum. We must note, however, that if we had reduced the perpendicular components of velocity of the cascade nuclei by the same factor of 2 we have applied to the forward component, we would have still been left with a large part of the disagreement.

The source of the remaining discrepancies between Calc-2 and experiment is not immediately clear. The calculated value of F/B is still too large, but the mean velocity at 15° is too low. If we recall Fig. 5, we can see that increasing the strength of the correlation between V and $v_{\parallel}$ while holding $\langle v_{\parallel} \rangle$ and the spectrum of V fixed tends to reduce F/B and increase $\langle V_{15°} \rangle$. Indeed, when we analyze $v_{\parallel}$ and V from Calc-2 in terms of the correlation equation [Eq. (9)], we find the mean value of n is only 0.045 in contrast to the value 0.44 deduced by the fitting procedure. That the calculated correlation is so weak is a consequence of the fact that the evaporation calculation predicts that V is independent of E^* (and hence $v_{\parallel}$) for a given evaporation-cascade length. The calculated correlation arises solely from there being a range of cascade lengths which contributes to forming a given product (see Fig. 9).

We can speculate that both of these fundamental differences between calculation and experiment are somehow connected with a role played by heavy fragments in "deep spallation" reactions. The prompt-cascade calculation in its present form treats only the ejection of nucleons and mesons. If heavy fragments such as Na^{24} are ejected at this step of the reaction, we expect that the remaining nucleus (the progenitor of Tb^{149}) will have reduced forward momentum, as there is evidence[12] for a preferred emission of Na^{24} in the forward direction in such reactions. It has been noted[38-40] that some aspects of heavy-fragment production can be accounted for in terms of an evaporation mechanism. Fragment production in such a process will

be a sensitive function of excitation energy and may serve to strengthen the V-E^* (or V-$v_{\parallel}$) correlation. Although the present work cannot prove a role for heavy fragments, it does point out substantial disagreements with existing calculations. It will be important to reanalyze the experimental data as improved calculations of the cascade and evaporation stages of the reaction become available.

B. Systematics of Velocities of "Deep Spallation" Products

Can we systematize the velocities of "deep spallation" products in such a way that will be useful in deciding whether a particular product is produced by "deep spallation" or fission, in a way that does not require detailed cascade-plus-evaporation calculations each time? We will consider an effective value of V [the $\Delta\vec{v}+\vec{V}$ in Eq. (10)] as arising from vector addition of a number of separate vectors; some from the "isotropic" part of the cascade step and some from the evaporation step. Where the final velocity V is imparted to the recoil in a series of isotropic steps, a random walk requires that

$$\langle V^2\rangle = \sum V_i^2 \,, \tag{12}$$

where V_i^2 is the average of the square of the velocity imparted to the recoil by the ith emitted particle. Momentum conservation requires that

$$M_i^2 V_i^2 = m_i^2 v_i^2 \,, \tag{13}$$

where the letter M denotes mass, with the upper-case symbols referring to the intermediate residual nucleus and the lower-case symbols referring to the emitted particle. The final mean-squared momentum of the observed nucleus is given by

$$\langle (M_{\rm obs}\, V)^2\rangle = M_{\rm obs}^2 \sum \left(\frac{m_i^2 v_i^2}{M_i^2}\right) . \tag{14}$$

If M_i can be approximated by the average of target and observed mass $\frac{1}{2}(M_t + M_{\rm obs})$, then

$$\langle (M_{\rm obs}\, V)^2\rangle = \frac{4M_{\rm obs}^2}{(M_t + M_{\rm obs})^2} \sum (m_i v_i)^2 \,. \tag{15}$$

The sum in turn may be replaced by $(M_t - M_{\rm obs}) \times \langle m_i^2 v_i^2\rangle$, where the average defines the average effective squared momentum kick per emitted nucleon. We then have

$$\langle m_i^2 v_i^2\rangle = \frac{(M_t + M_{\rm obs})^2 \langle \frac{1}{2} M_{\rm obs}\, V^2\rangle}{2M_{\rm obs}(M_t - M_{\rm obs})} \,. \tag{16}$$

As indicated above, the derivation of Eq. (16) has lumped any isotropic component of recoil from the prompt cascade together with that from the evaporation step. It is implicitly assumed that $\langle \frac{1}{2} M_{\rm obs}\, V^2\rangle$ exhibits very little dependence on bombarding energy.

For "deep spallation" of a given target, we expect that the average squared momentum per emitted nucleon, $\langle m_i^2 v_i^2\rangle$, will probably increase slowly with $M_t - M_{\rm obs}$. If one focuses on a given product and varies the target, a similar increase might occur. In general, as one considers different targets and products, he expects the individual values of m_i and v_i to change in some rather complex way depending on the prompt cascades, Coulomb barriers, binding energies, and the stastistics of nuclear level densities.

We have plotted in Fig. 10 $\langle m_i^2 v_i^2\rangle$ as a function of $M_t - M_{\rm obs}$ for a number of reactions that can reasonably be termed "deep spallation."[41] Included are the result from the present experiment, those for Tb^{149} production from Ta, Au, and Bi of Winsberg,[2] data for $Sc^{43,44}$, $Cu^{61,64}$, and Sr^{83} from Ag reported by Cumming *et al.*,[13] and Na^{24} production from V and Cu targets from the work of Porile and Tanaka.[42] The average recoil energy of the product [$\langle \frac{1}{2} M_{\rm obs}\, V^2\rangle$ in Eq. (16)] was taken from differential range spectra measured at 90° in the lab system, with the exception of those of Winsberg,[2] which are from 2π thin-target–thin-catcher measurements. The striking feature of Fig. 10 is that $\langle m_i^2 v_i^2\rangle$ depends primarily on $M_t - M_{\rm obs}$ and is not strongly dependent on the mass or charge of the target or prod-

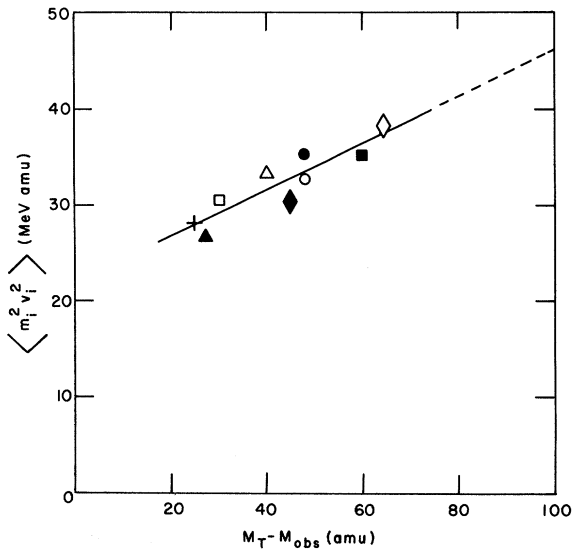

FIG. 10. Dependence of mean-square momentum per nucleon emitted $\langle m_i^2 v_i^2\rangle$ on the mass difference $M_t - M_{\rm obs}$ separating the product from the target. Points are for the following reactions: ● Tb^{149} from Au, present work; ○ Tb^{149} from Au, Ref. 2; ■ Tb^{149} from Bi, Ref. 2; □ Tb^{149} from Ta, Ref. 2; △ Na^{24} from Cu, Ref. 42; ▲ Na^{24} from V, Ref. 42; ◇ $Sc^{43,44}$ from Ag, Ref. 13; ◆ $Cu^{61,64}$ from Ag, Ref. 13; and + Sr^{83} from Ag, Ref. 13.

uct. This consistent trend of results for diverse reactions must indicate considerable cancellation or compensation of the various factors which determine the spectra and relative numbers of the emitted particles in the prompt and evaporation cascades. It has been concluded by Winsberg[2] that the mean recoil energy (and hence $\langle m_i^2 v_i^2 \rangle$) is independent of bombarding energy from 0.6 to 6 GeV. Comparison of the silver spallation study of Cumming *et al.*[13] at 2.9 GeV with that of Borisova *et al.*[43] at 0.48 GeV leads to the same conclusion. We have not included in Fig. 10 results for reactions in which $M_t - M_{obs}$ is less than 15. For simple spallation reactions, the prompt cascade may play a more important role, and our averaging procedures may not be valid. Indeed, the results of Panontin, Porile, and Caretto[44] on simple reactions in Ag and In targets, when analyzed in terms of Eq. (16), indicate an apparent increase in the value of $\langle m_i^2 v_i^2 \rangle$ for $M_t - M_{obs} \lesssim 10$.

It is possible to use the empirical correlation shown in Fig. 10 to characterize "deep spallation" and distinguish it from fission. To estimate where fission would fall in Fig. 10, we have applied Eq. (16) to the results obtained by Sugarman and coworkers[45,46] from recoil studies of the fission of U, Bi, and Ta by 0.45-GeV protons. As the resultant values of $\langle m_i^2 v_i^2 \rangle$ fall well off scale vertically in Fig. 10, they have been shown in Table VII. Even the lowest value 65 (MeV amu) for Ba^{128} from Ta^{181} is twice the value shown in Fig. 10 at the same $M_t - M_{obs}$. The large values of $\langle m_i^2 v_i^2 \rangle$ in Table VII reflect the dominant contribution in Eq. (12) of a single V_i to the observed recoil velocity, as expected in a fission process. General features of fission at moderate and high excitation energies, in particular the mean velocities of products, are predicted quite well by a liquid-drop model.[47] We would propose to use the correlation defined by the solid line in Fig. 10 and its dashed extension to characterize "deep spallation," and the liquid-drop model to characterize fission.

The most interesting region for such a distinction is for $80 < (M_t - M_{obs}) < 140$, because in this range the interaction of multi-GeV protons with uranium targets is known to give some products of high average recoil energy and some of low average recoil energy.[6,7,32,48,49] In particular, there is considerable interest in the rare-earth region, where a prominent double-peaked charge dispersion curve has been observed.[50,51] By extrapolation of the spallation systematics we would predict that the mean kinetic energy of Tb^{149} from a uranium target should be 7.7 MeV. From the range-energy relationship suggested by Hogan and Sugarman,[45] one obtains a mean range of 2.7 mg/cm^2 in uranium. By comparison, the liquid-drop model[39] gives ranges of 4.5–5.9 mg/cm^2 of uranium[52] for Tb^{149} produced by fission. Ranges of a neutron-excessive product, such as Nd^{147}, formed by fission will be even larger, 5.9–7.3 mg/cm^2 of uranium. The distinction between "spallation" as referred to Fig. 10 and "fission" as referred to liquid-drop calculations should be quite clear on the basis of range measurements.

Extrapolation of similar spallation systematics to products below the rare-earth region has led to the conclusion[9] that the momentum spectra of Ba^{131} and of Pd^{103} from uranium at 2.2 GeV include only small spallation contributions. In the iodine region, a mean range of 3.4 mg/cm^2 is predicted for I^{120} produced from uranium by spallation, while ranges of 7.5–8.7 mg/cm^2 are expected for I^{132} formed by fission. The measurements of Brandt[48] at 18 GeV and Alexander, Baltzinger, and Gazdik[6] at 3 and 6 GeV give values of $\approx$4 mg/cm^2 for neutron-deficient iodine isotopes and $\approx$8 mg/cm^2 for neutron-excessive ones. It has previously been concluded by Rudstam and Sorensen[10] on the basis of cross-section systematics that the neutron-deficient iodine isotopes are formed by "deep spallation" processes at 18 GeV and by a fissionlike process at 0.6 GeV. The systematics which we have developed gives added evidence for this classification of mechanisms.

An extensive study of products from Ta and U, now in progress,[53] will provide further information for comparison of processes expected to be primarily fission with processes expected to be primarily spallation.

IV. CONCLUSIONS

In starting this work, we had set as one of the goals the investigation of possible connections be-

TABLE VII. Mean square momentum per emitted nucleon, $\langle m_i^2 v_i^2 \rangle$ derived from observed kinetic energies of some products of the fission of U, Bi, and Ta by 0.45-GeV protons.

Target	Product	$M_t - M_{obs}$ (amu)	$\langle \frac{1}{2} M_{obs} V^2 \rangle$ (Ref. a) (MeV)	$\langle m_i^2 v_i^2 \rangle$ (MeV amu)
U^{238}	Nd^{147}	91	57.4	318
	Nd^{140}	98	47.7	248
Bi^{209}	Sr^{91}	118	61.0	256
	Pd^{109}	100	48.9	227
	Ba^{133m}	76	31.1	180
Ta^{181}	Cu^{67}	114	54.1	218
	Sr^{91}	90	45.6	206
	Pd^{109}	72	35.7	191
	Ba^{128}	53	9.25	65

[a] Values for the uranium targets obtained from Ref. 45. Those for bismuth and tantalum from Ref. 46.

tween "deep spallation" and fragment production in high-energy nuclear reactions. On examining the experimental data we find such a connection cannot be established uniquely, although it may well exist. The data are, within their errors, consistent with a two-step picture, there being no indication in the second step for a memory of the beam-direction effect such as was observed in a study of Na^{24} production from bismuth. It is only by quantitative comparison of the derived two-step parameters with model calculations, or by direct comparison of the experimental data with complete model calculations that we can hope to find evidence for fragmentation.

Such a comparison points out substantial disagreements between the experiment and the calculation when an intranuclear-nucleonic-cascade model is used which allows only the ejection of nucleons and mesons during the first step of the reaction, and the second step is described by a statistical model in which particles no heavier than Li^7 can be evaporated. Either we must abandon the two-step model and consider our finding a set of two-step parameters which can fit the observed data an accident, or we must modify the model calculations in such a way as to fit the data. Qualitatively, ejection of heavy fragments in the forward direction during the prompt-cascade step and emission of fragments heavier than Li^7 in the evaporation step would help explain the observed discrepancies, but this would again tend to connect Tb^{149} and fragment production.

What then is our picture of "deep spallation," fission, and fragmentation? How and/or why should we distinguish those events leading to Tb^{149} and a fragment from a fission? The most probable mass division in fission at high excitation energies is symmetric. Semiconductor-detector studies[31] of the fission of U and Bi by 2.9-GeV protons indicate a rapidly decreasing probability with increasing mass ratio for mass ratios ≈ 3. On the other hand, the mass-yield curve for heavy-element targets shows an upturn for masses below ≈ 40. This suggests the reverse trend, i.e., increasing probability for still more asymmetric mass divisions. A mass ratio of the order of 4 to 5 is perhaps a convenient experimental point at which to set the dividing line between fission and nonfission processes. In terms of the liquid-drop-model potential surface, fission corresponds to the passage of the system over a saddle point centered at symmetric mass division. There is presumably another saddle point centered at very asymmetric mass divisions which would, in a unified theory of fission and evaporation, account for emission of nucleons, α particles, etc. In very general terms, the existence of a potential peak between the two saddle points gives rise to low yields at intermediate mass ratios and forms the division between fission and nonfission. The fragments emitted in the "nonfission" or fragmentation events should have heavy partners. The fact that such a correlation has not yet been observed in counter experiments is probably due to currently feasible detection thresholds and requirements on angular acceptance.[31]

An empirical correlation is suggested for mean momentum per emitted nucleon in high-energy reactions of the "deep spallation" type. This appears to allow distinction between "deep spallation" and fission as formation mechanisms for products of high-energy nuclear reactions on the basis of mean-range measurements.

ACKNOWLEDGMENTS

The authors would like to express their appreciation to Dr. N. T. Porile for kindly performing the evaporation calculations discussed in the text. We are indebted to the group headed by R. Withnell for preparation of the targets and catcher foils. One of us (V.P.C.) wishes to acknowledge the hospitality of the Brookhaven National Laboratory Chemistry Department during the time he spent there. He would like to thank the Luso-American Educational Commission of Lisbon for a Fulbright grant and the University of Coimbra and the Portuguese Institute of Higher Culture for granting the leaves-of-absence.

---

*Research supported by the U. S. Atomic Energy Commission.

†Present address: Estudos Gerais Universtarios de Mozambique, Portugese, East Africa.

[1]R. B. Duffield and G. Friedlander, Brookhaven National Laboratory Report No. BNL-330, 1954 (unpublished), p. 27.

[2]L. Winsberg, Phys. Rev. 135, B1105 (1964).

[3]E. Bruninx, Nucl. Phys. 64, 481 (1965).

[4]E. M. Franz and G. Friedlander, Nucl. Phys. 76, 123 (1966).

[5]E. P. Steinberg, A. F. Stehney, C. Sterns, and I. Spaletto, Nucl. Phys. A113, 265 (1968).

[6]J. M. Alexander, C. Baltzinger, and M. F. Gazdik, Phys. Rev. 129, 1826 (1963).

[7]G. Friedlander, L. Friedman, B. Gordon, and L. Yaffe, Phys. Rev. 129, 1809 (1963).

[8]R. Wolfgang, E. W. Baker, A. A. Caretto, J. B. Cumming, G. Friedlander, and J. Hudis, Phys. Rev. 103, 394 (1956); A. A. Caretto, J. Hudis, and G. Friedlander, *ibid.* 110, 1130 (1958).

[9]V. P. Crespo, J. B. Cumming, and A. M. Poskanzer, Phys. Rev. 174, 1455 (1968).

[10]G. Rudstam and G. Sørensen, J. Inorg. Nucl. Chem.

29, 2515 (1966).
[11]A. M. Poskanzer, J. B. Cumming, and R. Wolfgang, Phys. Rev. 129, 374 (1963).
[12]J. B. Cumming, R. J. Cross, Jr., J. Hudis, and A. M. Poskanzer, Phys. Rev. 134, B167 (1964).
[13]J. B. Cumming, S. Katcoff, N. T. Porile, S. Tanaka, and A. Wyttenbach, Phys. Rev. 134, B1269 (1964).
[14]N. Sugarman, M. Campos, and K. Wielgoz, Phys. Rev. 101, 388 (1956).
[15]N. T. Porile and N. Sugarman, Phys. Rev. 107, 1410 (1957).
[16]L. Winsberg, University of California Radiation Laboratory Report No. UCRL-8618, 1958 (unpublished), p. 44; L. Winsberg and J. M. Alexander, in *Nuclear Chemistry*, edited by L. Yaffe (Academic Press Inc., New York, 1968), Vol. I, p. 340.
[17]L. P. Remsberg, Phys. Rev. 174, 1338 (1968).
[18]K. Ramavataram and D. I. Porat, Nucl. Instr. Methods 4, 239 (1959).
[19]J. M. Alexander and D. H. Sisson, Phys. Rev. 128, 2288 (1962).
[20]M. Kaplan and R. D. Fink, Phys. Rev. 134, B30 (1964).
[21]J. B. Natowitz and J. M. Alexander, Phys. Rev. 188, 1734 (1969).
[22]C. D. Moak and M. D. Brown, Phys. Rev. 149, 244 (1966).
[23]Exact solutions for nonzero values of b/a are:

$$\langle\langle V_L^2 \cos^2\theta_L\rangle\rangle = \langle v_\parallel^2 + \tfrac{1}{3}V^2(1+\tfrac{3}{5}b/a)/(1+b/3a)\rangle$$

and

$$\langle\langle V_L^2 \sin^2\theta_L\rangle\rangle = \langle v_\perp^2 + \tfrac{2}{3}V^2(1+b/5a)/(1+b/3a)\rangle .$$

[24]See J. M. Alexander, in *Nuclear Chemistry*, edited by L. Yaffe (Academic Press Inc., New York, 1968), Vol. I, p. 273; N. T. Porile, Phys. Rev. 185, 1371 (1969).
[25]N. Metropolis, R. Bivins, M. Storm, J. M. Miller, G. Friedlander, and A. Turkevich, Phys. Rev. 110, 204 (1958).
[26]L. P. Remsberg, Phys. Rev. 138, B572 (1965).
[27]N. T. Porile, Phys. Rev. 120, 572 (1960).
[28]K. Chen, Z. Fraenkel, G. Friedlander, J. R. Grover, J. M. Miller, and Y. Shimamoto, Phys. Rev. 166, 949 (1968).
[29]N. T. Porile and N. Sugarman, Phys. Rev. 107, 1422 (1957).
[30]Data from Ref. 4 have been corrected using the α-branching ratio reported by Y. Y. Chu, E. M. Franz, and G. Friedlander, Phys. Rev. 175, 1523 (1968).
[31]L. P. Remsberg, F. Plasil, J. B. Cumming, and M. L. Perlman, Phys. Rev. 187, 1597 (1969); Phys. Rev. C 1, 265 (1970).
[32]J. A. Panontin and N. T. Porile, J. Inorg. Nucl. Chem. 32, 1175 (1970).
[33]N. T. Porile and S. Tanaka, Phys. Rev. 135, B122 (1964).
[34]V. P. Crespo, J. M. Alexander, and E. K. Hyde, Phys. Rev. 131, 1765 (1963).
[35]The inelastic cross section of gold is estimated to be 1650 mb, from the review of R. W. Williams, Rev. Mod. Phys. 36, 815 (1964).
[36]G. Rudstam, Z. Naturfosch. 21, 1027 (1966).
[37]U. Schwarz and H. Oeschger, Z. Naturforsch. 22, 972 (1967).
[38]J. Hudis and J. M. Miller, Phys. Rev. 112, 1322 (1958).
[39]I. Dostrovsky, Z. Fraenkel, and J. Hudis, Phys. Rev. 123, 1452 (1961).
[40]I. Dostrovsky, R. Davis, Jr., A. M. Poskanzer, and P. L. Reeder, Phys. Rev. 139, B1513 (1965).
[41]A number of measurements have not been included in Fig. 10. These are measurements made by integral-range techniques (either with thick targets or with large angular acceptance) and those for which $M_t - M_{obs} < 15$. Differences in the inherent velocity averaging and in the range-energy relationships used makes inclusion of these measurements dubious.
[42]N. T. Porile and S. Tanaka, Phys. Rev. 137, B58 (1965).
[43]N. I. Borisova, M. Ya. Kuznetsova, L. N. Kurchatova, V. N. Mekhedov, and L. V. Chistyakov, Zh. Eksperim. i Teor. Fiz. 37, 366 (1959) [transl.: Soviet Phys.—JETP 10, 261 (1960)].
[44]J. A. Panontin, N. T. Porile, and A. A. Caretto, Jr., Phys. Rev. 165, 1281 (1968).
[45]J. J. Hogan and N. Sugarman, Phys. Rev. 182, 1210 (1969).
[46]N. T. Porile and N. Sugarman, Phys. Rev. 107, 1410 (1957).
[47]J. R. Nix and W. J. Swiatecki, Nucl. Phys. 71, 1 (1965).
[48]R. Brandt, *Physics and Chemistry of Fission* (International Atomic Energy Agency, Vienna, Austria, 1965), Vol. II, p. 329.
[49]E. Hagebo and H. Ravn, J. Inorg. Nucl. Chem. 31, 2649 (1969).
[50]Y. Y. Chu, E. M. Franz, G. Friedlander, and P. J. Karol, unpublished.
[51]K. Bächmann, unpublished.
[52]The variation in calculated mean ranges is due to the assumption of Bi^{203} or $U^{234.4}$ as the fissioning species in the calculation, see Ref. 9.
[53]J. B. Cumming, B. R. Erdal, B. Gatty, and P. J. Karol, unpublished.